Research Paper
Computational Methods for Differential Equations
http://cmde.tabrizu.ac.ir
Vol. 10, No. 2, 2022, pp. 461-474
DOI:10.22034/cmde.2021.42640.1834

Exact solutions and numerical simulation for Bakstein-Howison model

Elham Dastranj* **and Hossein Sahebi Fard**
Faculty of Mathematical Sciences, Shahrood university of technology, Shahrood, Semnan, Iran.

Abstract

In this paper, European options with transaction cost under some Black-Scholes markets are priced. In fact, stochastic analysis and Lie group analysis are applied to find exact solutions for European options pricing under considered markets. In the sequel, using the finite difference method, numerical solutions are presented as well. Finally, European options pricing are presented in four maturity times under some Black-Scholes models equipped with the gold asset as underlying asset. For this, the daily gold world price has been followed from Jan 1, 2016 to Jan 1, 2019 and the results of the profit and loss of options under the considered models indicate that call options prices prevent arbitrage opportunity but put options create it.

Keywords. Black-Scholes models; Transaction cost; Lie symmetries; Finite difference method.
2010 Mathematics Subject Classification.

1. Introduction

In financial literature, the pricing category is considered as one of the most important concepts. Contingent claims especially options are very good tools for reducing investment risk causing absorb of less risk-averse investors. The Black-Scholes model made a big progress in option pricing methodology. This model is one of the most reliable pricing models particularly for European options and it is used in many countries such as the Australian and French stock exchange. As known the Black-Scholes model, like any other model, considers some conditions in market where some cases are violated. Absence of transaction cost is an assumption which more observations of volatility of traded option valuations have exposed that this assumption is not realistic. In markets with transaction cost the formal Black-Scholes model is switched to a nonlinear one which is considered in this paper. In order to reach the purposes of this investigation, some instrumentals of stochastic analysis and Lie group analysis are applied. Recently, Lie group analysis is widely used in financial studies and can be seen in a lot of papers [6, 8, 9]. Also several studies have been conducted about pde solutions which can be seen in [1–3, 21].

In recent years, several financial studies have been conducted on options pricing. For example, in [9] power option pricing has been presented under fractional Heston model in the gold world market using fast Fourier transformation. In this paper, the study period has been classified to periods of three months and the profit and loss resulting from this option in each period have been calculated. In [7], power option pricing under two stochastic volatility models; double Heston model and double Heston with three jumps have been compared. This investigation indicates that the power option yields more premium income under the second considered model, double Heston with three jumps as well. Many nonlinear Black-Scholes models have been studied in the literature. In [12], analytic solutions for nonlinear and the Greek parameters are given. In [11], by reduction a nonlinear Black-Sholes model, a particular solution is presented. Hussain and Alrajhi in [16] used a genetic algorithm to find a numerical solution for the nonlinear Black-Sholes model. Mashayekhi and Hugger presented a finite difference scheme for a nonlinear Black-Sholes model with modified volatility [19].

Received: 04 November 2020 ; Accepted: 08 April 2021.
∗ Corresponding author. Email: elham.dastranj@shahroodut.ac.ir.

In this investigation several transaction cost models from the most relevant class of nonlinear Black-Scholes equations for European options are concerned. So consider two assets in the market, a liquid bond (risk-free asset) with an interest rate $r \geq 0$ and stock that is illiquid. Let (Ω, F, P) be a probability space that F_t is the filtration generated by the Brownian motion W_t at time t, $0 \leq t \leq T$ and P is the risk-neutral probability. In the transaction cost models, the dynamics of one share of underlying asset price S_t^0 at time t is

$$dS_t^0 = \mu S_t^0 + \sigma S_t^0 dW_t, \quad 0 \leq t \leq T, \tag{1.1}$$

where μ is drift and σ is volatility. The transaction price at time t is

$$S_t(\alpha) = e^{\rho\alpha} S_t^0, \tag{1.2}$$

when α shares are traded and $0 \leq \rho \leq 1$ is liquidity parameter [12].

Bakstein and Howison developed a parameterized model for liquidity effects arising from the trading in an asset. They tested and calibrated their model set-up empirically with high-frequency data of German blue chips and discussed further extensions of the model, including stochastic liquidity [4]. Their model is

$$\frac{\partial U}{\partial t} + \frac{1}{2}\sigma^2 S^2 \frac{\partial^2 U}{\partial S^2}\left(1 + 2\rho S \frac{\partial^2 U}{\partial S^2}\right) + rS\frac{\partial U}{\partial S} - rU = 0, \tag{1.3}$$

where $\rho \geq 0$ is liquidity parameter, σ is the volatility and r is the risk-free interest rate. Also for $r = 0$ the model is

$$\frac{\partial U}{\partial t} + \frac{1}{2}\sigma^2 S^2 \frac{\partial^2 U}{\partial S^2}\left(1 + 2\rho \frac{\partial^2 U}{\partial S^2}\right) = 0. \tag{1.4}$$

The above equation called Cetin et al.'s model [5].

The equations (1.3) and (1.4) have various set solutions, some of them are presented by using lie symmetries method in this paper. The quoted pde's have also approximated solutions that have been computed applying finite difference method.

In this paper two linear Black-Scholes models are considered in which two assets are assumed; a bond as risk-free and liquid asset and stock as illiquid. In this investigation with stochastic analysis and Lie group analysis instrumentals, exact solutions of European options pricing equipped transaction cost under considered models are presented. Then following the daily gold world price from Jan 1, 2016 to Jan 1, 2019, considering the gold 18 cutie as underlying asset and calculating the profit and loss of options under considered models. It has been shown that call options prices prevent arbitrage opportunity but put options create it.

This paper is outlined in 6 sections. In section 2 the basic concepts of Lie symmetries are given. Symmetry operators are found and some exact solutions for equations (1.3) and (1.4) are constructed by the reduction process. Section 3 is devoted to numerical solutions of equations (1.3) and (1.4) by finite difference method. Section 4 describes our methodology for the case study, the world gold market. The numerical solutions of option pricing with gold price in the world market are presented in section 5. The paper is concluded in section 6.

1.1. **Lie point symmetries.** Consider a system of differential equation with independent variables $x^i (1 \leq i < n)$ and dependent variable u of form

$$\Delta^s(x^i, u, u_i, u_{ij}, \dots) = 0, \quad 1 \leq s < k, \tag{1.5}$$

where $u_i = \frac{\partial u}{\partial x^i}$. The infinitesimal Lie transformation for considered equations are

$$\begin{aligned} \tilde{x}^i &\mapsto x^i + \epsilon\xi^i + \mathcal{O}(\epsilon^2), \\ \tilde{u} &\mapsto u + \epsilon\phi + \mathcal{O}(\epsilon^2), \end{aligned} \tag{1.6}$$

with a small parameter $\epsilon \ll 1$ and which leaves the system of equations invariant to $\mathcal{O}(\epsilon^2)$. Lie point symmetries correspond to the case where the infinitesimal generators $\xi^i = \xi^i(x_i, u)$ and $\phi = \phi(x_i, u)$ depend only on x^i and u and not on the derivatives or integrals of u. Generalized Lie symmetries are obtained in the case when the transformations (1.6) also depend on the derivatives or integrals of u. The infinitesimal transformations for the first and second derivatives to $\mathcal{O}(\epsilon^2)$ are given by the prolongation formula

$$\tilde{u}_i = u_i + \epsilon\zeta_i, \quad \tilde{u}_{ij} = u_{ij} + \epsilon\zeta_{ij}, \tag{1.7}$$

where

$$\zeta_i = D_i\hat{\phi} + \xi^s u_{si}, \quad \zeta_{ij} = D_i D_j\hat{\phi} + \xi^s u_{sij}, \tag{1.8}$$

and

$$\hat{\phi} = \phi - \xi^s u_s, \tag{1.9}$$

corresponds to the canonical Lie transformation for which $\tilde{x}^i = x^i$ and $\tilde{u} = u + \epsilon\tilde{\phi}$. The symbol D_i in (1.8) denotes the total derivative operator with respect to x^i. Similar formula to (1.8) can be applied for the transformation of the higher order derivatives. The condition for invariance of the DE system (1.5) to $\mathcal{O}(\epsilon^2)$ under the Lie transformation (1.6) can be expressed as

$$\mathcal{L}_v\Delta^s \equiv \tilde{v}(\Delta^s) = 0 \quad \text{where} \quad \Delta^s = 0, \quad 1 \le s \le k, \tag{1.10}$$

where

$$\tilde{v} = v + \zeta_i\frac{\partial}{\partial u_i} + \zeta_{ij}\frac{\partial}{\partial u_{ij}} + \dots \tag{1.11}$$

is the prolongation of the vector field

$$v = \xi^i\frac{\partial}{\partial x^i} + \phi\frac{\partial}{\partial u}, \tag{1.12}$$

associated with the infinitesimal transformation (1.6). The symbol $\mathcal{L}_v\Delta^s$ in (1.10) denotes the Lie derivative of Δ^s with respect to the vector field v (i.e., $\mathcal{L}_v\Delta^s = \frac{d\Delta^s}{d\epsilon}\big|_{\epsilon=0}$) [15].

Now consider $x_1 = x,\ x_2 = t$ and $s = 2$. The infinitesimal Lie transformations for these conditions are

$$\begin{aligned} x &\mapsto x + \epsilon\xi_1(x,t,u) + \mathcal{O}(\epsilon^2),\\ t &\mapsto t + \epsilon\xi_2(x,t,u) + \mathcal{O}(\epsilon^2),\\ u &\mapsto u + \epsilon\phi(x,t,u) + \mathcal{O}(\epsilon^2). \end{aligned} \tag{1.13}$$

The vector field associated with the above group of transformation can be written as

$$X = \xi_1(x,t,u)\frac{\partial}{\partial x} + \xi_2(x,t,u)\frac{\partial}{\partial t} + \phi(x,t,u)\frac{\partial}{\partial u}. \tag{1.14}$$

Because of the order of both equations (1.3) and (1.4), we need to apply the second prolongation of the operator (1.14) of the form [17]

$$X^{(2)} = X + \phi^x\frac{\partial}{\partial u_x} + \phi^t\frac{\partial}{\partial u_t} + \phi^{xx}\frac{\partial}{\partial u_{xx}} + \phi^{xt}\frac{\partial}{\partial u_{xt}} + \phi^{tt}\frac{\partial}{\partial u_{tt}}, \tag{1.15}$$

where ϕ^x, ϕ^t, ϕ^{xx}, ϕ^{xt} and ϕ^{tt} are prolongation coefficients written by

$$\begin{aligned} \phi^x &= D_x(\phi - \xi_1 u_x - \xi_2 u_t) + \xi_1 uxx + \xi_2 u_{xt},\\ \phi^t &= D_t(\phi - \xi_1 u_x - \xi_2 u_t) + \xi_1 uxt + \xi_2 u_{tt},\\ \phi^{xx} &= D_x(D_x(\phi - \xi_1 u_x - \xi_2 u_t)) + \xi_1 uxxx + \xi_2 u_{xxt},\\ \phi^{xt} &= D_x(D_t(\phi - \xi_1 u_x - \xi_2 u_t)) + \xi_1 uxxt + \xi_2 u_{xtt},\\ \phi^{tt} &= D_t(D_t(\phi - \xi_1 u_x - \xi_2 u_t)) + \xi_1 uxtt + \xi_2 u_{ttt}, \end{aligned}$$

where the operator D_x and D_t denote the total derivative with respect to x and t [14]. Using the standard Lie symmetry method, it can be concluded that equation (1.3) admits a 5-dimensional Lie group of symmetry spanned by the following infinitesimal generators,

$$\begin{aligned} &X_1 = \frac{\partial}{\partial t}, \quad X_2 = e^{rt}\frac{\partial}{\partial u}, \quad X_3 = x\frac{\partial}{\partial u}, \quad X_4 = x\frac{\partial}{\partial x} + u\frac{\partial}{\partial u},\\ &X_5 = xrt\frac{\partial}{\partial x} + t\frac{\partial}{\partial t} - \frac{-2x\ln x + (2 + (\sigma^2 + 2r)t)x + 8u(rt-1)\rho}{8\rho}\frac{\partial}{\partial u}. \end{aligned}$$

Similarly, equation (1.4) admits the operators

$$X_1^* = \frac{\partial}{\partial t}, \quad X_2^* = \frac{\partial}{\partial u}, \quad X_3^* = x\frac{\partial}{\partial u}, \quad X_4^* = x\frac{\partial}{\partial x} + u\frac{\partial}{\partial u},$$
$$X_5^* = x\frac{\partial}{\partial x} + t\frac{\partial}{\partial t} - \frac{x(\sigma^2 t + 2\ln x - 2)}{8\rho}\frac{\partial}{\partial u}$$

as the basis for symmetry generators.

1.2. **Reduction and exact solutions.** The first advantage of the symmetry group method is to construct new solutions from known solutions. To do this, the infinitesimals are considered and their corresponding invariants are determined. The Bakstein-Howison equation is expressed in the coordinates (x, t, u) to reduce this equation for searching its form in specific coordinates. Those coordinates will be constructed by searching for independent invariants (y, v) corresponding to an infinitesimal generator. So using the chain rule, the expression of the equation in the new coordinate allows us to the reduced equation. Here we will obtain some invariant solutions with respect to symmetries. First, we obtain the similarity variables for each term of the symmetries, then we use this method to reduce the equations and find the invariant solutions. As we see Lie point symmetries of equations (1.3) and (1.4) are determined by solving the overdetermining equation for the infinitesimal generators ξ_i and ϕ. Classical similarity solutions are obtained by requiring the solution surfaces for u which are mapped onto the same set of surfaces in the sense that $u'(x,t) = u(x,t)$. This condition yields the first-order partial differential equations $\xi_i u_i = \phi$ with characteristics given by the group trajectories [14],

$$\frac{dx^i}{d\varepsilon} = \xi_i, \qquad \frac{du}{d\varepsilon} = \phi. \tag{1.16}$$

Integrations of the group trajectories yield the invariants of the point Lie group admitted by the equation, and they may be used to construct the classical similarity solutions of equations. Some classical similarity solutions of the model including invariants are expected in the sequel.

1.2.1. *Reduced equations for (1.3).* In this part some reduced form and exact solutions of the equation (1.3) are given via the extracted invariants of some symmetries.

1. For generator X_1, the classical similarity solution of (1.3) is obtained by integrating the group of trajectories,

   $$\frac{dx}{d\varepsilon} = 0, \quad \frac{dt}{d\varepsilon} = 1, \quad \frac{du}{d\varepsilon} = 0,$$

   where ε is a parameter along the trajectories. The above integrations give $u = v(y)$, $t = y$ as the invariant transformations. Substituting $u = v(y)$ into (1.3), it is reduced to

   $$v' - rv = 0, \tag{1.17}$$

   with $v = Ce^{ry}$ as its solution. Consequently the group invariant solution is $u = Ce^{rt}$.
2. Consider the generator X_2. The classical similarity solution of (1.3) is obtained by integrating the group of trajectories,

   $$\frac{dx}{d\varepsilon} = x, \quad \frac{dt}{d\varepsilon} = 0, \quad \frac{du}{d\varepsilon} = u,$$

   where ε is a parameter along the trajectories. This system gives $u = v(y)$, $t = y$ as the invariant transformations. Inserting y into (1.3), leads to the trivial equation

   $$v = 0, \tag{1.18}$$

   with the trivial solution $u = 0$.

The one-parameter group for generator X_5 gives a non-trivial solutions obtaining from (1.18).
The flow $\exp(sX_5)(x,t,u) = (\bar{x},\bar{t},\bar{u})$ is

$$\bar{x} = xe^{rt(s-1)}, \qquad \bar{t} = te^s \tag{1.19}$$
$$\bar{u} = -\frac{\exp(rte^s - s)}{16\rho rt}\Big(t^2\exp(-rt+2s)\sigma^2 rx - r\sigma^2t^2xe^{-rt} + 2x\exp(-rt+2s)r^2t^2 - 2e^{-rt}r^2t^2x + 2x\ln(x)^2e^{-rt}$$
$$-2x\ln\left(x\exp\{rt(e^s-1)\}\right)^2 - 4xrte^{-rt} - 16urt\rho e^{-rt} + 4rtx\exp(-rt+s)\Big).$$

The substitution $u = Ce^{rt}$ in this flow gives the following non-trivial exact solution

$$\begin{aligned} u(x,t) = C\exp\{rt(e^s-1)+s+rx\} - \frac{xe^{rt-s}}{16\rho rt}\Big(&t^2\sigma^2 r\exp\{rt(1-e^{-s}-e^s)\} \\ &-r\sigma^2t^2e^{rt(1-e^{-s}-e^s)} + 2r^2t^2\exp\{rt(1-e^{-s}-e^s)-2s\} \\ &-2t^2r^2\exp\{rt(1-e^{-s}-e^s)\} + 2\ln\left(x\exp\{rte^{-s(e^s-1)}\}\right)^2\exp\{rt(1-e^{-s}-e^s)\} \\ &-2\ln\left(xe^{rt\exp\{-s(e^s-1)\}}\right)^2\exp\{rt(1-e^{-s}-e^s)\} \\ &-4rt\exp\{rt(1-e^{-s}-e^s)+s\} + 4rt\exp\{-rte^{-s}-s\}\Big). \end{aligned} \tag{1.20}$$

Also the substitution $u = 0$ in flow (1.19) gives the following non-trivial exact solution

$$\begin{aligned} u(x,t) = -\frac{xe^{rt-s}}{16\rho rt}\Big(&t^2\sigma^2re^{rt(1-e^{-s}-e^s)} - r\sigma^2t^2e^{rt(1-e^{-s}-e^s)} + 2r^2t^2e^{rt(1-e^{-s}-e^s)-2s} \\ &-2t^2r^2e^{rt(1-e^{-s}-e^s)} + 2\ln\left(xe^{rte^{-s(e^s-1)}}\right)^2e^{rt(1-e^{-s}-e^s)} \\ &-2\ln\left(xe^{rte^{-s(e^s-1)}}\right)^2e^{rt(1-e^{-s}-e^s)} - 4rte^{rt(1-e^{-s}-e^s)+s} + 4rte^{-rte^{-s}-s}\Big). \end{aligned} \tag{1.21}$$

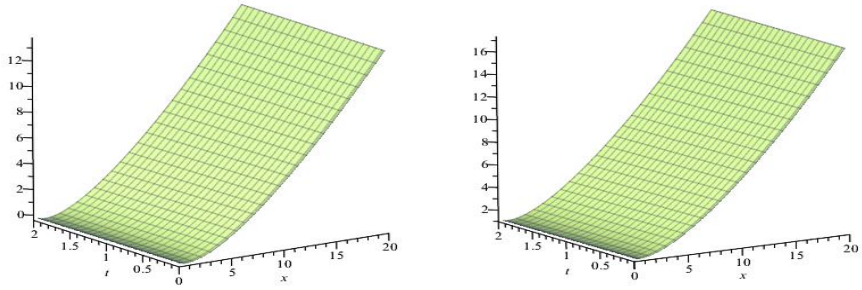

(a) Equation (1.20) (b) Equation (1.21)

FIGURE 1. Plots of solutions with European option conditions with $\sigma = 0.4,\ \rho = 0.6, r = 0.05$

See [20] for more details.

1.2.2. *Reduced equations for (1.4).* The same process is done in order to find some exact solution for equation (1.4).

1. For generator X_1^*, the classical similarity solution of (1.4) is obtained by integrating the group of trajectories,

$$\frac{dx}{d\varepsilon}=0, \qquad \frac{dt}{d\varepsilon}=1, \qquad \frac{du}{d\varepsilon}=0,$$

where ε is a parameter along the trajectories. The above integrations gives $u=v(y)$, $y=x$ as the invariant transformations. Substituting $u=v(y)$, into (1.4), it is reduced to

$$-\frac{1}{2}\sigma^2(2\rho r v''+1)r^2v''=0. \tag{1.22}$$

So, the reduced equation (1.22) gives two exact solutions

$$u(x,t)=-\frac{1}{2}\frac{x\ln(x)}{\rho}+\frac{1}{2}\frac{x}{\rho}+C_1x+C_2, \tag{1.23}$$

$$u(x,t)=C_1x+C_2. \tag{1.24}$$

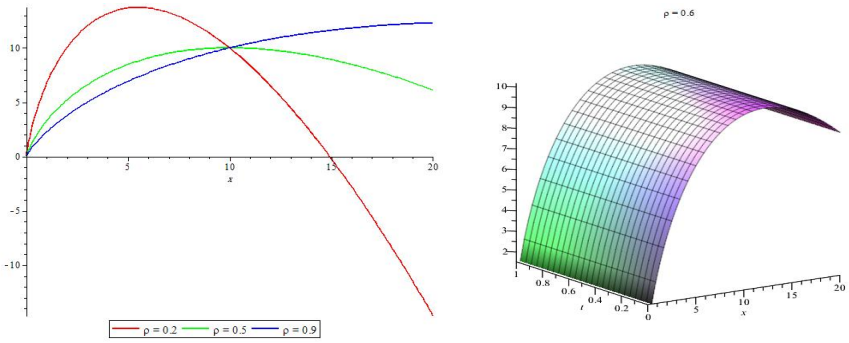

FIGURE 2. Plots of (1.23) for European option

Using the one-parameter group $\exp(sX_5^*)(x,t,u)=(\bar{x},\bar{t},\bar{u})$ for equation (1.4) yields

$$\bar{x}=xe^s, \qquad \bar{t}=te^s \tag{1.25}$$

$$\bar{u}=-\frac{te^{2s}\sigma^2x-\sigma^2tx+4x\ln(xe^s)e^s-4x\ln(x)-8xe^s-16u\rho+8x}{16\rho}.$$

The new solutions are obtained by substituting (1.23) and (1.24) into (1.25) as follows [20].

$$u(x,t)=-\frac{1}{2\rho}\left[(xe^{-s})\ln(xe^{-s})+xe^{-s}\right]+C_1xe^{-s}+C_2 \tag{1.26}$$

$$-\frac{te^{-2s}\sigma^2xe^{-s}-\sigma^2txe^{-s}+12xe^{-s}\ln(xe^{-s})e^{-s}-4xe^{-s}\ln(x)-8+8xe^{-s}}{16\rho},$$

and

$$u(x,t)=C_1xe^{-s}+C_2-\frac{te^{-2s}\sigma^2xe^{-s}-\sigma^2txe^{-s}+12xe^{-s}\ln(xe^{-s})e^{-s}-4xe^{-s}\ln(x)-8+8xe^{-s}}{16\rho}. \tag{1.27}$$

2. For another solution, consider the generator X_2^*. Thus, the classical similarity solution of (1.4) is obtained by integrating the group of trajectories,

$$\frac{dx}{d\varepsilon}=x, \qquad \frac{dt}{d\varepsilon}=0, \qquad \frac{du}{d\varepsilon}=u,$$

where ε is a parameter along the trajectories. The above integrations give $u=v(y)$, $x=\exp(q)$ and $t=y$ as the invariant transformations. Substituting these variables into (1.4),

$$v' \exp(q) = 0, \tag{1.28}$$

that yields the trivial solution

$$u = 0. \tag{1.29}$$

In order to find a non-trivial solution, the advantage of $\exp(sX_5^*)(x,t,u) = (\bar{x},\bar{t},\bar{u})$ is used again. This gives the following non-trivial solution

$$u(x,t) = \frac{te^{2s}\sigma^2 x - \sigma^2 tx + 4xse^s \ln x - 4x \ln x - 8xe^s + 8x}{16\rho}. \tag{1.30}$$

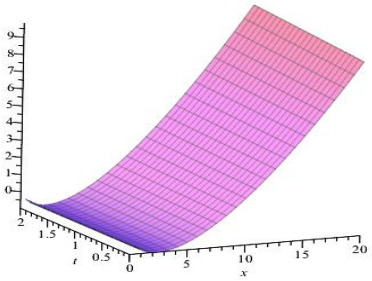

(a) Equation (1.26)

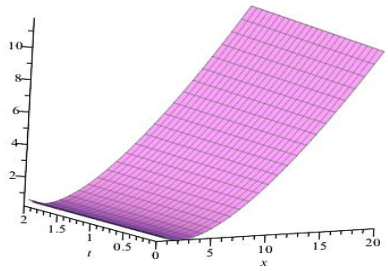

(b) Equation (1.27)

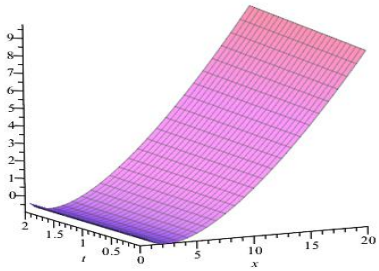

(c) Equation (1.30)

FIGURE 3. Plots of solutions with European option conditions with $\sigma = 0.4,\ \rho = 0.6$

2. Numerical solution

In this section, finite difference method is used to construct a numerical simulation for PDE (1.3) and (1.4). In relations (1.3) and (1.4), t denotes maturity time which decreases from T to zero. To simplify finite difference method calculations, by changing the variable t as $\tau(t) = T - t$, the backward equation has been transformed to a forward equation [10]. Note that τ increases from zero to T.

$$\frac{\partial U(S,t)}{\partial t} = \frac{\partial U(S,\tau(t))}{\partial \tau(t)}\tau'(t) = -\frac{\partial U(S,\tau)}{\partial \tau}. \tag{2.1}$$

By replacing $\tau(t)$ with t Bakstein and Howison's model is converted to

$$\frac{\partial U}{\partial t}-\frac{1}{2}\sigma^2S^2\frac{\partial^2U}{\partial S^2}\left(1+2\rho S\frac{\partial^2U}{\partial S^2}\right)-rS\frac{\partial U}{\partial S}+rU=0. \tag{2.2}$$

To solve (1.3), we divide the interval $[0,T]$ into M subintervals of length Δt. We also choose an upper bound (S_{max}) for S, for example, three or four times the value of the strike price. Now we divide $[0,S_{max}]$ to N subintervals of length δS. By this mesh, a grid point is denoted by $(n\Delta S, m\Delta t)$ where $n=0,1,\ldots,N$ and $m=0,1,\ldots,M$. Using an explicit method for the discretization of derivatives means a forward difference approximation for $\frac{\partial U}{\partial t}$ as

$$\frac{\partial U}{\partial t}(n\Delta S,m\Delta t)=\frac{u_n^{m+1}-v_n^m}{\Delta t}+O(\Delta t), \tag{2.3}$$

a central difference approximation for $\frac{\partial U}{\partial S}$ as

$$\frac{\partial U}{\partial S}(n\Delta S,m\Delta t)=\frac{u_{n+1}^m-u_{n-1}^m}{2\Delta S}+O((\Delta S)^2), \tag{2.4}$$

and a symmetric central difference approximation for $\frac{\partial^2U}{\partial S^2}$ as [10].

$$\frac{\partial^2U}{\partial S^2}(n\Delta S,m\Delta t)=\frac{u_{n+1}^m-2u_n^m+u_{n-1}^m}{(\Delta S)^2}+O((\Delta S)^2). \tag{2.5}$$

Now, we have

$$\frac{u_n^{m+1}-u_n^m}{\Delta t}-rn\Delta S\frac{u_{n+1}^m-u_{n-1}^m}{2\Delta S}+ru_n^m-\frac{1}{2}\sigma^2n^2(\Delta S)^2\frac{u_{n+1}^m-2u_n^m+u_{n-1}^m}{(\Delta S)^2}\left(1+2\rho n\Delta S\frac{u_{n+1}^m-2u_n^m+u_{n-1}^m}{(\Delta S)^2}\right)=0, \tag{2.6}$$

for $n=1,\ldots,N-1$ and $m=1,\ldots,M-1$. From (2.6) we get,

$$u_n^{m+1}=u_n^m+\frac{\sigma^2n^2\Delta t}{2}(u_{n+1}^m-2u_n^m+u_{n-1}^m)\left(1+2\rho n\frac{u_{n+1}^m-2u_n^m+u_{n-1}^m}{\Delta S}\right)+r\Delta tu_n^m-\frac{rn\Delta t}{2}(u_{n+1}^m-u_{n-1}^m), \tag{2.7}$$

and for Cetin et al.'s model (1.4) we obtain,

$$\frac{u_n^{m+1}-u_n^m}{\Delta t}-\frac{1}{2}\sigma^2n^2(\Delta S)^2\frac{u_{n+1}^m-2u_n^m+u_{n-1}^m}{(\Delta S)^2}\left(1+2\rho n\Delta S\frac{u_{n+1}^m-2u_n^m+u_{n-1}^m}{(\Delta S)^2}\right)=0, \tag{2.8}$$

for $n=1,\ldots,N-1$ and $m=1,\ldots,M-1$. From (2.8) we can get

$$u_n^{m+1}=u_n^m+\frac{\sigma^2n^2\Delta t}{2}(u_{n+1}^m-2u_n^m+u_{n-1}^m)\left(1+2\rho n\frac{u_{n+1}^m-2u_n^m+u_{n-1}^m}{\Delta S}\right). \tag{2.9}$$

In each time step the term u_n^{m+1} is evaluated from one time step back. Values $u_n^0,\ u_0^m,\ u_N^m$ for $n=1,\ldots,N,\ m=1,\ldots,M$ are known from initial and boundary conditions.

2.1. **Numerical examples.** In this subsection, we want to price some European options. The initial condition for European call option is $u(s,0)=\max(s-K,0),\ 0\le s\le S_{max}$, and boundary conditions are

$$\begin{cases}u(0,t)=0,\\ \frac{\lim_{s\to\infty}u(s,t)}{s}=1.\end{cases} \tag{2.10}$$

For put option, the initial condition is $u(s,0)=\max(K-s,0),\ 0\le s\le S_{max}$, and boundary conditions are

$$\begin{cases}u(0,t)=Ke^{-rt},\\ u(s,t)=0\quad for\ s\to\infty.\end{cases} \tag{2.11}$$

Let $\rho=0.6$ and $\sigma=0.4$ in Bakstein and Howison's model and take $r=0.05$. Let S_T is underlying asset price at maturity time. In Table 1 numerical results for (1.3) and (1.4) with finite difference method (FDM) and closed form, using "pdsolve" in Maple 18, are shown. The requirement parameters for finite difference method are $M=500$ and $N=10$. Table 1 shows that finite difference method and closed form have very close results.

TABLE 1. Comparison between finite difference method and closed form for $T = 1$ and $K = 10$

	Bakstein and Howison's model.		Cetin et al.'s model.	
	FDM	closed form	FDM	closed form
$S_T = 6$	0.569	0.45	0.48	0.36
$S_T = 9$	2.31	2.1	2.1213	1.98
$S_T = 12$	5.02	4.3	4.72	4.03
$S_T = 18$	12.31	10.3	11.89	10.002
$S_T = 24$	20.95	18.9	20.613	19
$S_T = 27$	25.48	22.7	25.26	24.9
CPU Time	0.007193	0.047	0.00622	0.015

Figure 4 shows FDM and closed form of a call option under this model. In Figure 5, FDM and closed form for Cetin et al.'s model are presented. As regards Figure 4 and Figure 5, the numerical solutions and closed form are very similar and their difference can be ignored.

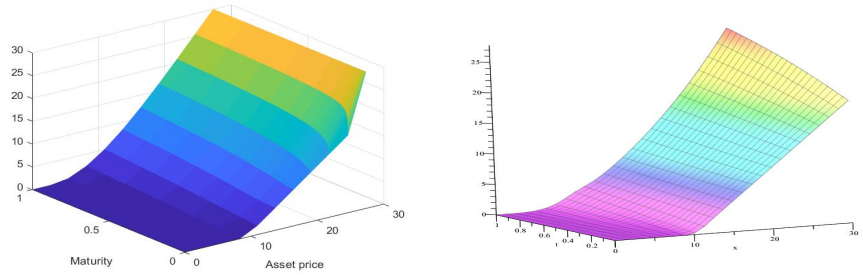

(a) FDM (b) Closed form

FIGURE 4. Finite difference method and closed form for Bakstein and Howison's model

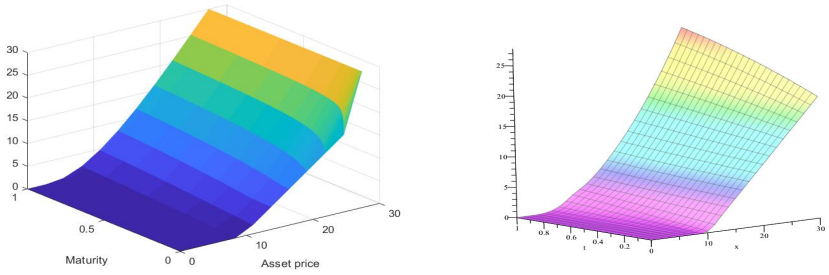

(a) FDM (b) Closed form

FIGURE 5. Finite difference method and closed form for Cetin et al.'s model.

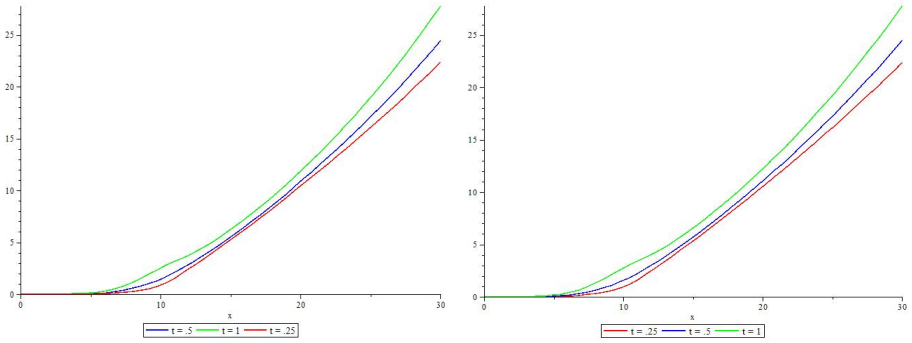

(a) Cetin et al.'s model (b) Bakstein and Howison's model

FIGURE 6. Call option pricing at some maturities when $K = 10$.

3. Methodology

In this paper, the underlying asset is the price of one Ounce gold in the world market. So the daily price of the considered underlying asset is observed from Jan 1, 2016 to Jan 1, 2019. For simplicity in calculation, all prices are reduced by 10^{-3}. Table 2 shows descriptive statistics of gold data in the considered period. It shows that the standard deviation and variance of 2019 are higher than other years. This volatility may create arbitrage opportunity for options in 2018 and this opportunity depends on option and strike price. This indicates the importance of option pricing and choosing an appropriate model. A good option price has a few profit, but a large profit of an option can create an arbitrage opportunity. Table 2 illustrates that the skewness is positive only in year 2018 which means this year has right-skewed distribution and other periods of study have left-skewed distribution. But measure of skewness in all periods are very low which shows that their distributions are not very asymmetry. Table 2 illustrates that the kurtosis is positive only for year 2017 as well. In other years, especially in years 2018 and 2019, kurtosis is too little.

TABLE 2. Descriptive statistics of underlying asset.

	2016	2017	2018	2019
Mean	1.24761	1.25931	1.26854	1.39834
Std. Deviation	0.07404	0.03443	0.05418	0.09289
Variance	0.005	0.001	0.003	0.009
Skewness	-0.537	-0.297	0.020	-0.030
Std. Error of Skewness	0.152	0.148	0.145	0.143
Kurtosis	-0.443	0.343	-1.525	-1.708
Std. Error of Kurtosis	0.303	0.295	0.289	0.285

To calculate liquidity parameter, the following formula has been used [13],

$$\rho = \frac{\text{Bid-Ask price}}{\text{Final trade price}}.$$

Pricing of European option with $T = 0.5$ and $T = 1$ at the beginning of 2017, 2018 and 2019 is our goal. In Table 3, the required parameters for options pricing are shown.

Table 3. Requirement parameters.

	2017	2018	2019
r	0.03	0.02	0.02
σ	0.07	0.03	0.05
ρ	0.007	0.01	0.002
S_0	1.209	1.316	1.281
S_T for $T = 0.5$	1.264	1.292	1.305
S_T for $T = 1$	1.316	1.281	1.517
K for $T = 0.5$	1.227	1.329	1.293
K for $T = 1$	1.245	1.342	1.306

4. Numerical results

Let C_1 (P_1), C_2 (P_2), and C_3 (P_3) be the Eorupean call (put) option with present spot at the beginning of year 2017, the beginning of year 2018 and the beginning of year 2019, respectively.

All six European options with two maturity times have been priced by using parameters quoted in Table 3. Figures 5 and 6 illustrate the changes of option price up to maturity time.

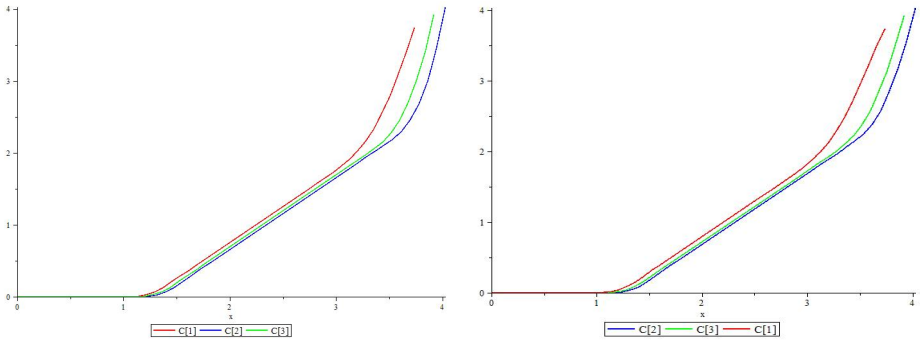

(a) Cetin et al.'s model (b) Bakstein and Howison's model

Figure 7. Call options pricing at $T = 1$.

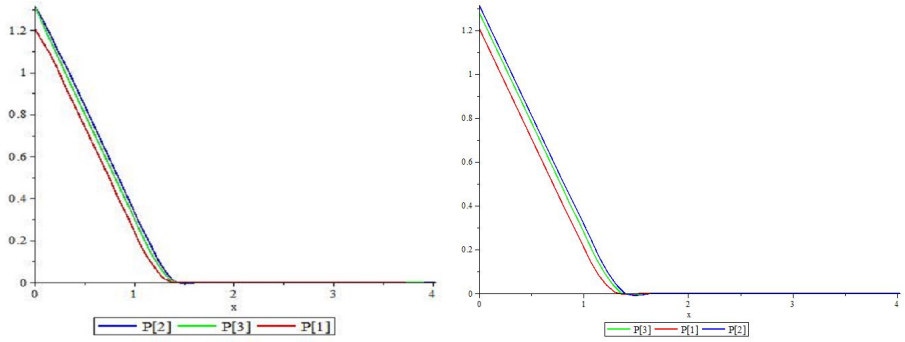

(a) Cetin et al.'s model (b) Bakstein and Howison's model

Figure 8. Put options pricing under at $T = 1$.

As is seen in Figures 7 and 8, option price has a jump if high volatility and intense increasing of underlying asset price happen at the same time. This jump may sound creator of an arbitrage opportunity, but option price controls the profit of option holder when the underlying asset price goes up. In Figure 9, pricing option of C_1 under Cetin et al.'s model and Bakstein and Howison's model by changing $K \in [0.8, 1.8]$ and $T \in [0, 1]$ is shown. As is shown in Figure 9, the price of options is very close under both models, also in option pricing, some jumps appear. Figure 9 shows that the price of option rapidly increases at short maturities but the increasing speed become slower after three months maturity or more.

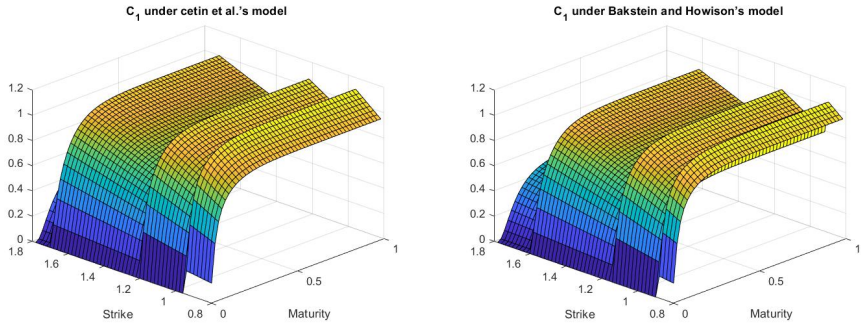

(a) Cetin et al.'s model (b) Bakstein and Howison's model

FIGURE 9. Pricing C_1 with changing K and T.

In the sequel, the profit of considered options are given by using the real price of asset at maturity time (Table 3). As is known, call option is used when the strike price is less than the real price of the underlying asset in the maturity time. Otherwise, the future price of call option becomes holder loss. The future price of option is equal to the cost that the holder pays for the option. If call option is applied, the profit can be seen as,

$$\text{Profit} = \text{real price} - \text{strike price} - \text{future option price}.$$

Similarly, the put option is used when the strike price is more than the real price of underlying asset in the maturity time and otherwise the future price of put option becomes holder loss. If put option is applied, the profit can be seen as below,

$$\text{Profit} = \text{strike price} - \text{real price} - \text{future option price}.$$

According to Table 3, C_1, C_3 and P_2 are applied and P_1, P_3 and C_2 are not used. In Table 4, the results of option pricing are shown. Columns "Profit" indicate profit of option for it's holder.

Table 4. Numerical results

		Bakstein and Howison's model		Cetin et al.'s model	
Option type		Price	Profit	Price	Profit
C_1	T=0.5	0.7335	-0.71874	0.7334	-0.73684
	T=1	0.747	-0.69875	0.747	-0.69875
C_2	T=0.5	0.1428	-0.14313	0.1403	-0.14568
	T=1	0.3057	-0.30647	0.3004	-0.31188
C_3	T=0.5	0.629	-0.62879	0.6281	-0.62971
	T=1	0.7536	-0.55742	0.7532	-0.55782
P_1	T=0.5	0.0033	-0.003	0.0034	-0.0034
	T=1	0.00001	-0.00001	0.00001	-0.00001
P_2	T=0.5	0.5319	-0.51319	0.5393	-0.50565
	T=1	0.4735	-0.43288	0.4841	-0.42207
P_3	T=0.5	0.1639	-0.16854	0.1652	-0.16721
	T=1	0.0346	-0.03581	0.0351	-0.0353

As is shown in Table 4, the price of options under two models are really near. For all options, profits are negative, which means the holder of option not only gets no profit but also loses. In fact, the option holder loses as much as option price, if he/she does not use the option. The holder gets no profit, if he/she uses the option because of high price of option. So there exists no arbitrage opportunity for option holder. It can be imagined that in this option pricing, the option holder loses and seller of option gets an arbitrage profit and the models are not suitable for this option pricing. But note that the profit of the option seller consequently is just as much as the price of option, and as a result, the models have good results to prevent arbitrage opportunity for option holder as well.

5. Conclusion

Investment in gold market is in high risk due to high volatility of this market. So future price forecast in this market is too difficult. Using options is one of the best methodologies for reducing risk and creating a more secure place for investment. Finding appropriate price for options is a big challenge in option pricing. Because the option profit in a market with high volatility can create an arbitrage opportunity and consequently makes the market more unsecured for investment, choosing of appropriate model, especially in markets with transaction cost, is an effective factor on suitable pricing. In this paper, investigating of the two models shows that these two models with appropriate pricing of European option not only hedge the market risk, but also prevent arbitrage opportunity.

6. Acknowledgment

We thank the anonymous reviewers for their careful reading of our manuscript and their many insightful comments and suggestions. The authors also thank Shahrood university of technology for its financial support of this research under project No: 23100.

References

[1] M. B. Almatrafi, A. R. Alharbi, and C. Tunç, *Constructions of the soliton solutions to the good Boussinesq equation*, Advances in Difference Equations 2020, *1* (2020), 1-14.

[2] M. Al-Asad, M. N. Alam, C. Tunç, and M. M. A. Sarker, *Heat Transport Exploration of Free Convection Flow inside Enclosure Having Vertical Wavy Walls*, Journal of Applied and Computational Mechanics, (2020). DOI: 10.22055/jacm.2020.35381.2646.

[3] M. N. Alam and C. Tunç, *New solitary wave structures to the (2+ 1)-dimensional KD and KP equations with spatio-temporal dispersion*, Journal of King Saud University-Science, *32*(8) (2020), 3400-3409.

[4] D. Bakstein and S. Howison, *A non-arbitrage liquidity model with observable parameters for derivatives*, working paper, Oxford center for industrial and applied mathematics, Oxford, *1-52* (2003).

[5] U. Cetin, R. Jarrow, and P. Protter, *Liquidity risk and arbitrage pricing theory*, Finance Stoch., *8* (2004), 311-341.
[6] E. Dastranj and S. R. Hejazi, *New Solutions for Fokker-Plank Equation of Special Stochastic Process via Lie Point Symmetries*, Computational Methods for Differential Equations, *5*(1) (2017), 30-42.
[7] E. Dastranj and R. Latifi, *A comparison of option pricing models*, international journal of financial engineering, February 21, (2017),4.02n03, 1750024.
[8] E. Dastranj and S. R. Hejazi, *Exact solutions for Fokker-Plank equation of geometric Brownian motion with Lie point symmetries*,Computational Methods for Differential Equations, *6*(3) (2018), 372-379.
[9] E. Dastranj and et al., *Power option pricing under the unstable conditions (Evidence of power option pricing under fractional Heston model in the Iran gold market)*, Physica A: Statistical Mechanics and its Applications, *537: 122690* (2020).
[10] G. Dura and A. M. Moşneagu, *Numerical approximation of Black-Scholes equation*, Annals of the AlexandruIoan-Cuza University-Mathematics, *56*(1) (2010), 39-64.
[11] J. E. Esekon, *A particular solution of a nonlinear Black-Scholes partial differential equation*, International Journal of Pure and Applied Mathematics, *81*(5) (2012), 715-721.
[12] J. E. Esekon, *Analytic solution of a nonlinear Black-Scholes equation*, International Journal of Pure and Applied Mathematics, *82*(4) (2013), 547-555.
[13] M. J. Fleming and E. M. Remolona, *Price formation and liquidity in the U.S. Treasury market: The response to public information*, The Journal of Finance, *54*(5) (1999), 1901-1915.
[14] S. R. Hejazi, *Lie group analysis, Hamiltonian equations and conservation laws of Born–Infeld equation*, Asian-European Journal of Mathematics, *7*(3) (2014), 1450040.
[15] S. R. Hejazi, *Lie point symmetries, Hamiltonian equation and conservation laws of the geodesics on a Schwarzschild Black hole*, Kragujevac Journal of Mathematics, *42*(3) (2014), 453–475.
[16] E. A. Hussain and Y. M. Alrajhi, *Numerical Solution of Nonlinear Black–Scholes Equation by Accelerated Genetic Algorithm*, Mathematical Theory and Modeling, *5*(4) (2015), 53-66.
[17] E. Lashkarian, S. R. Hejazi, N. Habibi, and A. Motamednezhad, *Symmetry properties, conservation laws, reduction and numerical approximations of time-fractional cylindrical-Burgers equation*, Communications in Nonlinear Science and Numerical Simulation, *67* (2019), 176-191.
[18] E. Lashkarian, E. Saberi, and S. R. Hejazi, *Symmetry reductions and exact solutions for a class of nonlinear PDEs*, Asian-European Journal of Mathematics, *9*(2) (2016), 1650061.
[19] S. Mashayekhi and J. Hugger, *Finite difference schemes for a nonlinear Black-Scholes model with transaction cost and volatility risk*, Acta Mathematica Universitatis Comenianae, *84*(2) (2015), 255-266.
[20] P. J. Olver, *Applications of Lie groups to differential equations*, Springer Science and Business Media, *107* (2000).
[21] C. Tunc, C. Islam, M. Alam, and M. Al-Asad, *An analytical technique for solving new computational of the modified Zakharov-Kuznetsov equation arising in electrical engineering*, Journal of Applied and Computational Mechanics, (2020). DOI: 10.22055/jacm.2020.35571.2687.